HHS Public Access

Author manuscript

Oncogene. Author manuscript; available in PMC 2018 July 26.

Published in final edited form as:

Oncogene. 2018 April ; 37(15): 2052–2066. doi:10.1038/s41388-017-0051-9.

CHTM1, a novel metabolic marker deregulated in human malignancies

Mansi Babbar[1], **Ying Huang**[1], **Jie An**[1], **Steve K. Landas**[2], and **M. Saeed Sheikh**[1]

[1]Department of Pharmacology, SUNY Upstate Medical University, Syracuse, New York 13210

[2]Department of Pathology, SUNY Upstate Medical University, Syracuse, New York 13210

Abstract

A better understanding of the link between cellular metabolism and tumorigenesis is needed. Here, we report characterization of a novel protein named Coiled-coil Helix Tumor and Metabolism 1 (CHTM1). We have found that CHTM1 is associated with cancer and cellular metabolism. CHTM1 localizes to mitochondria and cytosol, and its deficiency in cancer cells results in decreased mitochondrial oxygen consumption and ATP levels as well as oxidative stress indicating mitochondrial dysfunction. CHTM1-deficient cancer cells display poor growth under glucose/glutamine-deprived conditions, whereas cells expressing increased levels of exogenous CHTM1 exhibit enhanced proliferation and survival under similar conditions. CHTM1 deficiency also leads to defects in lipid metabolism resulting in fatty acid accumulation, which explains poor growth of CHTM1-deficient cells under glucose/glutamine deprivation since nutrient deprivation increases dependency on lipids for energy generation. We also demonstrate that CHTM1 mediates its effect via the PKC, CREB and PGC-1alpha signaling axis, and cytosolic accumulation of CHTM1during nutrient deprivation appears to be important for its effect on cellular signaling events. Furthermore, analyses of tissue specimens from 71 breast and 97 colon cancer patients show CHTM1 expression to be upregulated in the majority of tumor specimens representing these malignancies. Collectively, our findings are highly significant because CHTM1 is a novel metabolic marker that is important for the growth of tumorigenic cells under limiting nutrient supplies and thus, links cellular metabolism and tumorigenesis.

Keywords

Breast cancer; Colon cancer; Cell metabolism; CHCHD5; CREB; Mitochondrial dysfunction; PGC-1 alpha; PKC

Corresponding Author: M. Saeed Sheikh, M.D., Ph.D., Department of Pharmacology, SUNY Upstate Medical University, 750 E Adams St. Syracuse, NY 13210, Phone: 315-464-8015, sheikhm@upstate.edu.

Conflicts of Interests: The authors declare no competing financial interests.

Introduction

It is now well-established that normal cells predominantly depend on oxidative phosphorylation (OXPHOS) for energy generation, whereas cancer cells rely on aerobic glycolysis. Given that glycolysis is less efficient pathway to generate energy, cancer cells by undergoing the metabolic switch from OXPHOS to glycolysis may conceivably acquire a state that facilitates their rapid proliferation[3, 24]. This switching, commensurate to the rapid proliferation of cancer cells, involves complex metabolic reprogramming but the molecular details remain to be fully elucidated.

Various transcription factors and cofactors have been reported to regulate cellular metabolism including CREB (cAMP response element binding protein)[17]. CREB, a transcription factor, regulates cellular metabolism in response to various stresses, and its function is regulated via phosphorylation at Ser133 by various kinases [11, 21, 27, 29]. CREB has various targets including PPAR gamma coactivator-1 alpha (PGC-1α). PGC-1α is a master regulator of mitochondrial biogenesis[16, 17] and linked to various metabolic disorders[3]. It is also involved in metabolic switch from glucose to fatty acid oxidation (FAO)[20].

Recent studies have shown that glucose depletion makes cancer cells more dependent on OXPHOS and FAO for energy generation. Defects in OXPHOS and FAO increase cancer cell sensitivity to glucose deprivation[1, 7]. Clearly, cancer can also be considered as a metabolic disorder; thus, a better understanding of the alterations in cellular metabolism linked to tumorigenesis is needed to improve the management of human malignancy. In the present study, we report the characterization of a novel protein that is named Coiled-coil Helix Tumor and Metabolism 1 (CHTM1) based on its features reported in this manuscript. Sequence corresponding to CHTM1 is also annotated in the databank as CHCHD5, an experimentally uncharacterized protein of unknown function based on the predicted presence of two CHCH domains [4]. Our present study demonstrates that CHTM1 is a novel metabolic marker that is deregulated in human malignancies and plays an important role in promoting the growth of tumorigenic cells under limiting nutrient supplies. Thus, our results are highly significant, and provide valuable new information about the link between altered cellular metabolism and the process of tumorigenesis.

Results

CHTM1 localizes to cytosol and mitochondria

Fig. 1A shows the nucleotide and amino acid sequences for human CHTM1. The human *CHTM1* gene harbors four exons (Fig. 1A) that encode a protein of 110 amino acids with a molecular mass of 12.9 kDa. CHTM1 is predicted to harbor two coiled coil helix-coiled coil helix (CHCH) domains (Fig. 1A) and is evolutionarily conserved, sharing high degree of homology with its counterparts from various species (Fig. S1A). It is also predicted to be phosphorylated at serine, threonine and tyrosine residues, with the highest probability of being phosphorylated at serine 29 (Fig S1B). CHTM1 antibodies, generated against full-length recombinant CHTM1, specifically detected the recombinant CHTM1 protein (Fig. 1B, left panel) and exogenous CHTM1 protein (Fig. 1B, middle panel). CHTM1 antibodies

also detected the endogenous CHTM1 in the expected size range (~13 kDa); the CHTM1 shRNAs targeting three different regions of CHTM1 mRNA significantly reduced CHTM1 levels (Fig. 1B, right panel) further confirming the anti-CHTM1 antibody specificity.

To determine the subcellular localization of CHTM1, we performed immunostaining on MCF-7 human breast cancer cells. Results (Fig. 1C) indicated a punctate staining pattern and diffuse background staining for CHTM1. The punctate staining overlapped with that of mitochondrial-specific mitotracker suggesting CHTM1 to be mitochondrial, whereas its diffuse staining suggested cytosolic distribution. Biochemical analyses performed using cytosolic and mitochondrial fractions prepared from UACC-62 cells (Fig. 1D) and MCF-7 and 293T cells (Fig. S1C&D) revealed that CHTM1 was present in both cytosol and mitochondria. Because CHTM1 was also detected in mitochondria, sucrose gradient centrifugation was performed to determine its sub-mitochondrial localization[2]. The submitochondrial fractions representing outer membrane (OM), inter-membrane space (IMS), inner membrane (IM) and matrix were analyzed by Western blotting. The results indicated that, unlike other mitochondrial proteins such as VDAC, CHCM1 and Hsp60, CHTM1 was predominantely detected in the IMS similar to Smac (Fig. 1E) a known IMS protein[5].

CHTM1 regulates mitochondrial function and cellular sensitivity to glucose/glutamine deprivation

Mitochondrial distribution of CHTM1 prompted us to investigate its potential influence on mitochondrial function. Fig. 2A shows CHTM1-deficient MCF-7 cells exhibiting decreased oxygen consumption rate, suggesting reduced oxidative phosphorylation. CHTM1-deficient MCF-7 cells also demonstrated decreased cellular and mitochondrial ATP levels when compared to scrambled cells (Fig. 2B). Reduction in ATP is known to activate AMPK (AMP-activated protein kinase) activity[15], accordingly, CHTM1 knockdown in MCF-7 cells enhanced AMPK phosphorylation (Fig. 2C). Collectively, these results indicate that CHTM1 deficiency leads to mitochondrial dysfunction. Because oxidative phosphorylation is tightly coupled with glycolysis, we also measured lactate levels to determine CHTM1 effect on glycolysis. CHTM1-deficient cells showed increased lactate levels in the media (Fig. S2A), suggesting increased glycolysis. Because mitochondrial dysfunction has been linked to oxidative stress[10], the effect of CHTM1 deficiency on oxidative stress was also investigated. DCF-DA, a reactive oxygen species (ROS) sensitive dye, was used for measuring cellular ROS in CHTM1 knockdown cells. The results (Fig. 2D) revealed that CHTM1-deficient cells had significantly increased ROS levels indicating oxidative stress. Together, these results indicate that CHTM1-deficiency affects mitochondrial function.

Defects in electron transport chain[12] and mitochondrial activity[19] have been linked to altered cellular sensitivity to glucose deprivation. Likewise, cancer cells are believed to also rely on glutamine, a non-essential amino acid, for energy generation[14]. Because CHTM1 knockdown affected mitochondrial function, we therefore, investigated the effect of CHTM1-deficiency on cellular sensitivity to glucose/glutamine deprivation using MCF-7 and UACC-62 cells. Because pyruvate is an important product of glucose via glycolysis and the fact that cells can also utilize glutamine for energy generation through the TCA cycle,

CHTM1 knockdown and scrambled (control) cells were cultured under glucose, glutamine and sodium pyruvate-deprived conditions. The growth behavior of cells grown under these conditions was analyzed by phase contrast microscopy, crystal violet staining and trypan blue exclusion assays. We noted that while CHTM1 knockdown in MCF-7 cells (Fig. S2B) and CHTM1 overexpression in RKO cells (Fig. S2C) did not significantly alter cell proliferation and survival in complete culture medium, both CHTM1-deficient MCF-7 cells (Fig. 2E&F) and UACC-62 cells (Fig. S2D, E&F) grew poorly under glucose/glutamine-deprived conditions when compared to their respective scrambled counterparts (Fig. 2E&F and Fig. S2B, C&D). Conversely, cell proliferation and survival were significantly enhanced in CHTM1-overexpressing RKO colon cancer cells (that inherently exhibit low levels of endogenous CHTM1) compared to RKO cells expressing the empty vector-only under the glucose/glutamine-deprived conditions (Fig. 2G&H). Together, these results indicate that CHTM1 levels affect mitochondrial function, and cell proliferation and survival under nutrient (glucose/glutamine)-deprived conditions.

CHTM1 regulates cellular lipid metabolism

Our preceding results indicate that CHTM1-deficient cells exhibited poor growth and survival under nutrient (glucose/glutamine)-deprived conditions suggesting their inability to utilize alternative sources (such as lipids) to generate energy for their survival under such conditions. To determine whether indeed that was the case, we investigated the lipid metabolism in CHTM1-proficient and -deficient cells. Our results (Fig. 3A and Fig. S3) revealed that the lipid droplets, indicated by BODIPY staining, were more abundant in most of the CHTM1-deficient MCF-7 and UACC-62 cells grown in complete media or glucose/glutamine-deprived media. We also performed the Oil Red O (ORO) staining to detect neutral lipids in CHTM1-proficient and -deficient cells and the results (Fig. 3B) showed that CHTM1 deficiency was also associated with increased ORO staining indicating increased cellular lipid content (p value =0.0171). Conversely, overexpression of CHTM1 in MCF-7 cells led to a decrease in lipid droplet accumulation (Fig. 3C, left panel) as well as ORO staining (Fig. 3C, right panel, p value =0.0351) under glucose/glutamine-deprived conditions indicating decreased cellular lipid content. Together, these results indicate that CHTM1 regulates intracellular lipid accumulation in both the presence and absence of glucose/glutamine, and that CHTM1-deficient cells appear to have defects in lipid metabolism. Thus, CHTM1-deficient cells are capable of growing in the glucose/glutamine-containing medium because they do not depend on lipids for energy generation under these conditions. However, since CHTM1-deficient cells appear to have defects in lipid metabolism, they exhibit poor growth under glucose/glutamine-deprived conditions because glucose/glutamine deprivation increases dependency on lipids for energy generation.

Increased lipid accumulation in CHTM1-deficient cells could occur due to increased lipogenesis or decreased lipolysis. To gain insight into these alternatives, we analyzed genes linked to fatty acid oxidation or synthesis. As shown in Fig. 3D, CHTM1 knockdown caused a decrease in the expression of various genes linked to fatty acid oxidation including carnitine palmitoyltransferase 1b (CPT1b), medium-chain acyl-CoA dehydrogenase (MCAD) and peroxisome proliferator-activated receptor alpha (PPAR-α). Interestingly, CHTM1 knockdown in MCF-7 cells was also associated with a decrease in the expression of

genes involved in fatty acid synthesis, which included acetyl-CoA carboxylase 1 (ACC1), fatty acid synthase (FAS), sterol regulatory element-binding protein-1c (SREBP-1c) and peroxisome proliferator-activated receptor gamma (PPAR-γ) (Fig. 3E). Similar regulation of genes linked to fatty acid oxidation and synthesis was also noted under the glucose/glutamine-deprived conditions (data not shown). It is possible that the decrease in fatty acid synthesis as reflected by decreased expression of genes involved in fatty acid synthesis in CHTM1-deficient cells, could be a feedback mechanism in response to decreased fatty acid oxidation or increased lipid accumulation. We also performed the reverse experiments by overexpressing CHTM1 in MCF-7 cells and noted that increased levels of exogenous CHTM1 caused increased expression of genes involved in fatty acid oxidation and fatty acid synthesis (data not shown). Collectively, these results suggest that CHTM1 is an important player involved in the regulation of lipid metabolism.

CHTM1 regulates PPAR gamma coactivator-1 alpha (PGC-1α)

Next, we investigated the possible mechanisms via which CHTM1 regulated genes involved in fatty acid metabolism. Given that PGC-1α is a transcription coactivator that is known to play a key role in regulation of glucose and fatty acid metabolism[8], we investigated the potential influence of CHTM1 on PGC-1α. Our results indicated that CHTM1 knockdown resulted in down-regulation of endogenous PGC-1α levels in MCF-7 (Fig. 4A) and UACC-62 (Fig. 4B) cells grown in complete culture medium or the glucose/glutamine-deprived medium. We also performed the reverse experiments using RKO and MDA-231 cells that exhibit low levels of endogenous CHTM1 and noted that stable expression of exogenous CHTM1 led to increased PGC-1α levels (Fig. 4C). Together, these results indicate that CHTM1 regulates endogenous PGC-1α levels. To confirm that alterations in PGC-1α levels were also reflected in changes in PGC-1α activity, the expression of PGC-1α downstream target genes including Pyruvate dehydrogenase kinase 4 (PDK4) and Carnitine palmitoyltransferase-1b (CPT-1b) were analyzed. Our results indicated that PGC-1α down-regulation due to CHTM1 knockdown was also coupled with down-regulation of PDK4 and CPT-1b mRNA levels (Fig. 4D); Western blotting confirmed that down-regulation of PDK4 mRNA was coupled with a decrease in PDK4 protein levels (Fig. 4E). Thus, CHTM1 deficiency affects both PGC-1α levels and function. We also investigated the effect of CHTM1 overexpression on PGC-1α mRNA and its downstream target genes, and the results showed that CHTM1 overexpression led to increased mRNA expression of PGC-1α and its downstream target genes, CPT1b and PDK-4 (Fig. 4F). Because CHTM1 deficiency or overexpression-mediated regulation of PGC-1α also occurred at the mRNA levels, next, we investigated CHTM1 effect on PGC-1α promoter activity. We used PGC-1α promoter-reporter construct co-expressed with CHTM1 or control vector in MCF-7 cells; results (Fig. 4G) showed exogenous CHTM1 to upregulate PGC-1α promoter activity. Thus, CHTM1 regulates PGC-1α at the transcriptional level and could also affect lipid metabolism, in part, via its influence on PGC-1α expression.

CHTM1 regulates CREB phosphorylation via Protein Kinase C (PKC)

CREB transcription factor is known to be activated via phosphorylation on Ser133 and regulates PGC-1α transcription under energy stress conditions. CREB transcriptionally regulates PGC-1α gene expression via the CREB-binding element present within the

promoter of PGC-1α gene[13]. Next, we investigated whether CHTM1 was involved in CREB activation. We noted that both MCF-7 and UACC-62 cells exhibited constitutive phosphorylation of CREB at Ser133 in complete medium or glucose/glutamine-deprived medium (Fig. 5A&B scrambled controls). Interestingly, CHTM1 knockdown in both cell lines resulted in decreased CREB phosphorylation on Ser133; the effect was more pronounced under glucose/glutamine-deprived conditions (Fig. 5A&B). CHTM1 knockdown also led to a significant reduction in the transactivation function of CREB from its regulatory element (Fig. 5C). Thus, reduction in CREB phosphorylation due to CHTM1 deficiency was functionally relevant, as it was also reflected in decreased CREB transactivation function. Our results indicate that CHTM1 regulates CREB activity and that CHTM1 is expected to regulate PGC-1α (as shown in Fig. 4) at least in part via CREB.

Various kinases such as PKA, PKC PI3K and p38 have been implicated in phosphorylation and activation of CREB. To identify the kinase(s) engaged by CHTM1 to regulate CREB phosphorylation on Ser133, we investigated the effects of various kinase inhibitors on CHTM1-mediated increase in CREB phosphorylation. Our results indicated that PKC inhibitor abrogated CHTM1-mediated CREB phosphorylation ($p=0.0844$), whereas PKA, PI3K and p38 inhibitors did not (Fig. 5D). Consistent with these results, phorbol 12-myristate 13-acetate (PMA), known to activate PKC, rescued CHTM-1 deficiency-mediated decreases in CREB phosphorylation, whereas the PKA activator forskolin, and oleic acid (an unsaturated fatty acid) did not (Fig. 5E). These results suggest that CHTM1-mediated increase in CREB phosphorylation involves PKC activity.

Glucose/glutamine deprivation increases cytosolic distribution of CHTM1

We also sought to investigate how CHTM1 affects cellular signaling during glucose/glutamine deprivation. We found that while the total endogenous CHTM1 protein levels were not significantly changed during glucose/glutamine-deprived conditions (Fig. 6A, lanes 1&2 and 5&6), the cytosolic levels of endogenous CHTM1 were increased (Fig. 6A, lanes 3&4 and 7&8). We also analyzed RKO cells stably expressing exogenous CHTM1 and noted increased cytosolic accumulation of exogenous CHTM1 under glucose/glutamine-deprived conditions (data not shown). Thus, cytosolic accumulation of both the endogenous and exogenous CHTM1 is regulated in a similar manner under glucose/glutamine deprived conditions. Furthermore, increased accumulation of cytosolic CHTM1 was specific to glucose/glutamine deprivation because treatment with other agents such as H_2O_2, metformin or oxamate did not have similar effect (Fig. 6B). We also examined the effect of exogenous CHTM1 on the cytosolic levels of phospho-CREB under glucose/glutamine-deprived conditions, and found that increased CHTM1 levels in cytosol were also coupled with increased cytosolic phospho-CREB (Fig. 6C). Blots were also probed for cytosolic protein α-tubulin, and mitochondrial protein Sam50 as positive and negative controls (Fig. 6A, B&C). Together these results suggest that cytosolic accumulation of CHTM1 during nutrient (glucose/glutamine) deprivation appears to be important for its effect on cellular signaling events particularly in relation to its impact on CREB function.

CHTM1 is overexpressed in patient samples of breast and colon cancers

Given that cancer can also be considered as a metabolic disease, therefore, we investigated the expression of CHTM1 in human malignancy. To that end, we analyzed samples representing matching normal and tumor tissues from patients with breast and colon cancers. CHTM1 levels were determined by Western blot and immunohistochemical analyses. Fig. 7A depicts a representative Western blot showing results from 6 pairs of colon cancer samples and as is shown, tumor samples from all patients exhibited increased levels of CHTM1 when compared to their corresponding matched normal tissues. Overall, we analyzed matched normal and tumor tissue from 53 colon cancer patients by Western blotting and found 43 out of 53 (81.11%) tumors to show increased levels of CHTM1 when compared to matched normal tissues (Fig. S4, Fig. S5A and Table S1). We also sought to analyze CHTM1 status in tumors by immunohistochemical staining and to that end first confirmed the specificity of anti-CHTM1 antibody using scrambled and CHTM1-knockdown cells. Our results (Fig. S5B, left panel) confirmed that the anti-CHTM1 antibody detected the immunohistochemistry-based signals in the scrambled cells but not in CHTM1-knockdown cells. Furthermore, only the anti-CHTM1 antibody detected endogenous CHTM1 signals, whereas isotype matched IgG did not (Fig. S5B, right panel). After confirming that the anti-CHTM1 antibody specifically detected CHTM1, we analyzed 44 colon cancer patient samples by immunohistochemical staining and our results indicated that 36 out of 44 (81.81%) tumors exhibited increased levels of CHTM1 (Table S2). Representative results showing increased staining for CHTM1 in tumor tissues are depicted in Fig. 7B.

In the case of breast cancer, samples from 10 patients were analyzed by Western blotting and all 10 breast cancer samples showed increased levels of CHTM1 when compared to corresponding matched normal tissues (Fig. S6 and Table S3). Representative results of 6 pairs of matched normal and tumor tissues are shown in Fig. 7C. In the case of immunohistochemical analyses, out of 61 informative cases, 51 (about 83.60%) tumors had increased staining for CHTM1 (Table S4). Representative results showing increased staining for CHTM1 in tumor tissues are depicted in Fig. 7D. Overall results for colon and breast cancer samples are summarized in Fig. 7E. We also investigate the CHTM1 expression status in microarray data in the GEO database. CHTM1 expression data for 17 colorectal cancer patients (GEO profile ID # GSD4382) were retrieved that indicated CHTM1 mRNA expression to be higher in tumors compared to matching normal tissues (Fig. 7F). Together these results indicate that CHTM1 is overexpressed in human colon and breast cancers.

Discussion

We report, for the first time, the experimental characterization of CHTM1. Database searches revealed the presence of cDNAs corresponding to CHTM1 as experimentally uncharacterized protein. We provide experimental evidence that CHTM1 is detected in both mitochondria and cytosol, and in the case of mitochondria, predominantly in the inter-membrane space (IMS). Furthermore, CHTM1deficiency affects mitochondrial function and its levels alter cellular growth under nutrient (glucose/glutamine) deprivation. For example, CHTM1 deficiency led to defective OXPHOS coupled with reduced ATP production

indicating defects in mitochondrial function. We noted that CHTM1-deficient cells grown in the complete medium exhibited enhanced glycolysis as was evident by increased lactate production. Possibly, CHTM1-deficient cells with defective mitochondrial function grown in the complete medium increasingly rely on enhanced glycolysis for proliferation and survival. CHTM1-deficient cells, however, exhibited poor growth in the glucose/glutamine-deprived conditions suggesting that CHTM1-deficient cells were unable to utilize alternative sources to generate energy for their proliferation and survival. Because glucose/glutamine deprivation leads to metabolic stress, these findings also suggest that CHTM1 appears to function as an important modulator of cellular response to metabolic stress. In this context, it is of note that metabolic stress induces fatty acid oxidation for ATP generation[9]. However, the CHTM1-deficient cells exhibit defects in lipid metabolism. For example, CHTM1 deficiency under regular and nutrient (glucose/glutamine)-deprived conditions was associated with increased intracellular lipid contents, while reverse was noted upon overexpression of CHTM1. Furthermore, CHTM1 knockdown was associated with decreased expression of genes involved in fatty acid oxidation as well as those involved in fatty acid synthesis. In the reverse experiments, overexpression of CHTM1 was also associated with increased expression of genes involved in fatty acid oxidation and fatty acid synthesis. Conceivably, alteration in fatty acid synthesis is a feedback response to changes in fatty acid oxidation because both fatty acid synthesis and oxidation are coupled processes. Thus, alterations in CHTM1 levels appear to regulate lipid metabolism affecting both lipogenesis and lipolysis. Accordingly, due to defects in lipid metabolism, the CHTM1-decifient cells would be compromised in generating ATP via fatty acid oxidation following metabolic stress.

We also noted that CHTM1-deficient cells had an increased rate of protein catabolism under glucose/glutamine deprived conditions as was evident by higher levels of urea production by these cells (Fig. S7). These results coupled with the finding that CHTM1-deficient cells exhibit increased glycolysis would be consistent with the notion that CHTM1-deficient cells, unable to fully metabolize lipids, switch to increased utility of carbohydrates and proteins for energy generation. This would also explain that despite defects in mitochondrial function and lipid metabolism, the CHTM1-deficient cells are capable of growing in the regular medium i.e. in the presence of glucose/glutamine. This scenario will be similar to that reported for another mitochondrial protein namely, CHCHD4/MIA40 (Ref [28]). CHCHD4/MIA40-deficient cells have been reported to grow normally under normoxia, however, their growth is affected under hypoxic conditions. It has also been reported that cancer cells harboring *PIK3CA* mutations exhibit normal growth in complete medium but do not grow optimally under glutamine-deprived conditions[14].

Our results also indicate that CHTM1 regulates PGC-1α levels and activity. PGC-1α is a transcriptional co-activator that regulates downstream targets that are linked to modulating fatty acid metabolism. Our results further indicate that CHTM1 affects PGC-1α regulation at the transcriptional level. CHTM1 is not predicted to function as a transcription factor and thus, unlikely to directly affect transcription of PGC-1α. In this context, involvement of CREB appears to be more likely for the following reasons: (i) CREB has been known to regulate PGC-1α transcription under metabolic stress, (ii) the PGC1 α promoter harbors CREB binding site (CRE), (iii) alterations in CHTM1 levels lead to changes in CREB

phosphorylation and activity that are coupled with changes in PGC-1α levels and (iv) CREB phosphorylation at Ser133 is a critical step in its activation accordingly, CHTM1 appears to engage PKC to induce CREB phosphorylation at Ser133. Although CREB is reported to induce PGC-1 α and repress PPAR-γ during FAO[17], our results indicate that decreased CREB activity was associated with a decrease in both PGC-1 α and PPAR-γ in CHTM1 knockdown cells. PPAR-γ down-regulation may conceivably reflect a feedback response to changes in lipogenesis or is independent of CREB regulation. CREB has been reported to positively regulate PGC-1 α expression[17], which further positively regulates PPAR-γ expression[25], suggesting an indirect positive correlation between CREB activity and PPAR-γ regulation.

In addition to mitochondria, CHTM1 was detected in cytosol. Interestingly, cytosolic accumulation of CHTM1 was more pronounced under glucose/glutamine-deprived conditions. Retrograde signaling from mitochondria to cytosol has been reported to be linked to nutrient sensing and stress response[6]. Increased cytosolic CHTM1 may reflect translocation from mitochondria to cytosol as a consequence of nutrient stress response. Alternatively, increased cytosolic levels of CHTM1 may reflect de novo synthesis or increased stability of CHTM1 in cytosol in response to nutrient stress. Although further studies are needed to elucidate these alternatives, cytosolic accumulation of CHTM1 is clearly indicative of an important and novel feature of metabolic stress response. Furthermore, increased cytosolic accumulation of CHTM1 during nutrient (glucose/glutamine) deprivation is coupled with increased cytosolic levels of phospho-CREB (active-CREB). Thus, cytosolic accumulation of CHTM1 appears to be functionally relevant in context to its effect on cellular signaling events particularly in relation to CREB.

We have also analyzed matched normal and tumor tissues from colon and breast cancer patients. Our results indicate that the majority of tumors have increased levels of CHTM1 when compared to matching normal tissues. Given that cancer is also considered as a metabolic disease, the significance of these findings is relevant to the process of tumorigenesis and metastasis. For example, it is conceivable that increased levels of CHTM1 during transformation would promote the growth of tumorigenic cells particularly under limiting nutrient supplies. Likewise, early in the process of tumorigenesis when angiogenesis is not fully established, the increasing levels of CHTM1 would also enable the transformed cells to better adapt to and survive under the limiting nutrient supplies. Consistent with this notion, it has been reported that tumors in the advanced and metastatic stages show increased dependency on mitochondrial respiration and fat consumption[18, 23, 26]. Accordingly, our results are highly significant because CHTM1 is a novel metabolic marker that appears to play an important role in promoting the growth of tumorigenic cells under limiting nutrient supplies and thus, links cellular metabolism and tumorigenesis. Therefore, targeting CHTM1 appears to be a viable approach to halt the growth of advanced and metastatic tumors. Based on our collective results, we propose (Fig. 8) CHTM1 to be a novel and important modulator of cellular response to metabolic stress that appears to mediate its effect, at least in part, via the PGC-1α, CREB and PKC signaling axis. Furthermore, CHTM1 is deregulated in human malignancies and could potentially serve as an important tumor marker that can also be developed as a target of novel anticancer therapeutics.

Materials and methods

Antibodies and reagents

Antibodies: anti-HA tag (clone 3F10) (Roche Applied Science), anti-β-actin and anti-alpha-tubulin (Sigma-Aldrich), anti-Smac (Upstate Cell Signaling Solutions, Lake Placid, NY), anti-Hsp60 (Enzo Life Sciences, Plymouth Meeting, PA), anti-VDAC1 (Calbiochem, Darmstadt, Germany), anti-GAPDH, anti-PDK4 and anti-Vinculin (Santa Cruz), anti-PGC-1α (a gift from Dr. Daniel P. Kelly, Sanford-Burnham Medical Research Institute, FL), anti-pAMPK, anti-pCREB and anti-CREB (Cell Signaling Technologies, Boston, MA), anti-CHCHD4 (Protein-Tech Group, IL), anti-Tim23 (BD Biosciences, San Diego, CA). The peroxidase-conjugated goat anti-rat, goat anti-rabbit, goat anti-mouse and horse anti-goat antibodies were from Vector Laboratories (Burlingame, CA). Rabbit polyclonal antibodies specific for human CHTM1 were generated in our laboratory through ProSci Inc. (Poway, CA) using full-length recombinant human CHTM1 protein purified from *Escherichia coli*. For cell transfections, Mirus (Madison, WI) and Lipofectamine 2000 (Invitrogen, Carlsbad, CA) were used. Restriction endonucleases were from New England BioLabs (Ipswich, MA). PKA inhibitor-H89, p38 inhibitor-SB203580, PI3K inhibitor-LY294002 and PKC inhibitor-GO6983 were from Sigma-Aldrich (St. Louis, MO). Other chemical reagents were from Thermo Fisher Scientific and Sigma-Aldrich.

Cells and culture conditions

Human cell lines HEK293T (embryonic kidney cells from NIH), MCF-7 (breast cancer cells from NIH), RKO (human colon cancer cells from NIH), MDA-MB-231 (breast cancer cells from NIH), UACC-62 (melanoma cells from Dr. Markovitz, University of Michigan) were maintained in Dulbecco's modified Eagle's medium (DMEM) supplemented with 10% fetal bovine serum (Gemini Bio-Products, West Sacramento, CA). For glucose/glutamine deprivation experiments, cells were washed 3 times with PBS and incubated with DMEM without glucose, glutamine and sodium pyruvate.

Expression constructs

pCMV6-CHTM1 construct was purchased from Origene, MD. ORF of *CHTM1* was inserted into pSRα-HA-S and pCEP4 expression vectors for transient and stable expression respectively. GST-tagged CHTM1 was generated by inserting the PCR-amplified full-length CHTM1 cDNA into pGEX6P-1 expression vector (GE Healthcare, Pittsburgh, PA). All expression vectors were sequenced to validate their authenticity.

Luciferase assays

pGL3-PGC-1α promoter construct was a gift from Dr. Michael Shuen (York University, Canada). pFA2-CREB and pFR-Luc (Agilent, Santa Clara, CA) were used to measure CREB activity. Luciferase assays were performed as previously reported [22]

Oxygen consumption rate, ATP and extracellular lactate measurement

Whole cell oxygen consumption rate was measured by an Oxygraph system (Hansatech Instruments, Norfolk, UK) as described previously[2]. ATP and lactate levels were measured

using kits from Promega (Madison, WI) and Enzo Life Sciences (Farmingdale, NY) per the manufactures' protocols.

Western blotting, immunostaining, immunohistochemistry and cell fractionation

Western blotting and immunostaining were done as previously described[2]. Band intensities were measured using Image J program. Immunohistochemistry staining was performed using Vector Vectastain kit per the manufacturer's protocol. Photomicrographs were captured using Olympus AX70 fluorescent microscope. Mitochondrial and cytosolic fractionations were done as previously described[2].

Human Biological samples

Samples for western blot analyses were from Cooperative Human Tissue Network, an NCI-supported network. Frozen samples were shipped on dry-ice and kept at -80˚C for long-term storage. Samples for immunohistochemistry were purchased from Biomax (Rockville, MD) as formalin-fixed, paraffin-embedded tissue array slides. Slides were shipped and stored at room temperature. Quantification was performed by a pathologist.

Statistical analysis

All experiments represent at least three-independent repeats. Values are mean ± S.E. Statistical significance was determined by a 1-tailed or 2-tailed Student's t test or ANOVA. The value of $p < 0.05$ was considered as statistically significant.

Supplementary Material

Refer to Web version on PubMed Central for supplementary material.

Acknowledgments

We thank Dr. Daniel P. Kelly, Sanford-Burnham Medical Research Institute, FL for providing the anti-PGC-1α antibody and Dr. Michael Shuen, York University, Ontario, Canada for pGL3-PGC-1α promoter construct. Dr. David M. Markovitz (Department of Internal Medicine, University of Michigan Medical Center) kindly provided UACC-62 melanoma cells (originally from Dr. Maria S. Soengas, Melanoma Laboratory, Spanish National Cancer Research Center). This work was supported in part by Carol M. Baldwin breast cancer fund and NIH grant CA150132.

References

1. Agarwal NR, Maurya N, Pawar JS, Ghosh I. A combined approach against tumorigenesis using glucose deprivation and mitochondrial complex 1 inhibition by rotenone. Cell Biol Int. 2016; 40:821–831. [PubMed: 27109893]
2. An J, Shi J, He Q, Lui K, Liu Y, Huang Y, et al. CHCM1/CHCHD6, novel mitochondrial protein linked to regulation of mitofilin and mitochondrial cristae morphology. J Biol Chem. 2012; 287:7411–7426. [PubMed: 22228767]
3. Babbar M, Sheikh MS. Metabolic Stress and Disorders Related to Alterations in Mitochondrial Fission or Fusion. Mol Cell Pharmacol. 2013; 5:109–133. [PubMed: 24533171]
4. Banci L, Bertini I, Ciofi-Baffoni S, Jaiswal D, Neri S, Peruzzini R, et al. Structural characterization of CHCHD5 and CHCHD7: two atypical human twin CX9C proteins. J Struct Biol. 2012; 180:190–200. [PubMed: 22842048]

5. Burri L, Strahm Y, Hawkins CJ, Gentle IE, Puryer MA, Verhagen A, et al. Mature DIABLO/Smac is produced by the IMP protease complex on the mitochondrial inner membrane. Mol Biol Cell. 2005; 16:2926–2933. [PubMed: 15814844]
6. Butow RA, Avadhani NG. Mitochondrial signaling: the retrograde response. Mol Cell. 2004; 14:1–15. [PubMed: 15068799]
7. Buzzai M, Bauer DE, Jones RG, Deberardinis RJ, Hatzivassiliou G, Elstrom RL, et al. The glucose dependence of Akt-transformed cells can be reversed by pharmacologic activation of fatty acid beta-oxidation. Oncogene. 2005; 24:4165–4173. [PubMed: 15806154]
8. Canto C, Auwerx J. PGC-1alpha, SIRT1 and AMPK, an energy sensing network that controls energy expenditure. Curr Opin Lipidol. 2009; 20:98–105. [PubMed: 19276888]
9. Carracedo A, Cantley LC, Pandolfi PP. Cancer metabolism: fatty acid oxidation in the limelight. Nat Rev Cancer. 2013; 13:227–232. [PubMed: 23446547]
10. Cui H, Kong Y, Zhang H. Oxidative stress, mitochondrial dysfunction, and aging. J Signal Transduct. 2012; 2012:646354. [PubMed: 21977319]
11. Delghandi MP, Johannessen M, Moens U. The cAMP signalling pathway activates CREB through PKA, p38 and MSK1 in NIH 3T3 cells. Cell Signal. 2005; 17:1343–1351. [PubMed: 16125054]
12. Fath MA, Diers AR, Aykin-Burns N, Simons AL, Hua L, Spitz DR. Mitochondrial electron transport chain blockers enhance 2-deoxy-D-glucose induced oxidative stress and cell killing in human colon carcinoma cells. Cancer Biol Ther. 2009; 8:1228–1236. [PubMed: 19411865]
13. Fernandez-Marcos PJ, Auwerx J. Regulation of PGC-1alpha, a nodal regulator of mitochondrial biogenesis. Am J Clin Nutr. 2011; 93:884S–890. [PubMed: 21289221]
14. Hao Y, Samuels Y, Li Q, Krokowski D, Guan BJ, Wang C, et al. Oncogenic PIK3CA mutations reprogram glutamine metabolism in colorectal cancer. Nat Commun. 2016; 7:11971. [PubMed: 27321283]
15. Hardie DG. AMP-activated protein kinase: an energy sensor that regulates all aspects of cell function. Genes Dev. 2011; 25:1895–1908. [PubMed: 21937710]
16. Herzig S, Long F, Jhala US, Hedrick S, Quinn R, Bauer A, et al. CREB regulates hepatic gluconeogenesis through the coactivator PGC-1. Nature. 2001; 413:179–183. [PubMed: 11557984]
17. Herzig S, Hedrick S, Morantte I, Koo SH, Galimi F, Montminy M. CREB controls hepatic lipid metabolism through nuclear hormone receptor PPAR-gamma. Nature. 2003; 426:190–193. [PubMed: 14614508]
18. Kamarajugadda S, Stemboroski L, Cai Q, Simpson NE, Nayak S, Tan M, et al. Glucose oxidation modulates anoikis and tumor metastasis. Mol Cell Biol. 2012; 32:1893–1907. [PubMed: 22431524]
19. Landor SK, Mutvei AP, Mamaeva V, Jin S, Busk M, Borra R, et al. Hypo- and hyperactivated Notch signaling induce a glycolytic switch through distinct mechanisms. Proc Natl Acad Sci U S A. 2011; 108:18814–18819. [PubMed: 22065781]
20. Lehman JJ, Kelly DP. Transcriptional activation of energy metabolic switches in the developing and hypertrophied heart. Clin Exp Pharmacol Physiol. 2002; 29:339–345. [PubMed: 11985547]
21. Li B, Kaetzel MA, Dedman JR. Signaling pathways regulating murine cardiac CREB phosphorylation. Biochem Biophys Res Commun. 2006; 350:179–184. [PubMed: 16996475]
22. Lucchesi C, Sheikh MS, Huang Y. Negative regulation of RNA-binding protein HuR by tumor-suppressor ECRG2. Oncogene. 2016; 35:2565–2573. [PubMed: 26434587]
23. Luo X, Cheng C, Tan Z, Li N, Tang M, Yang L, et al. Emerging roles of lipid metabolism in cancer metastasis. Mol Cancer. 2017; 16:76. [PubMed: 28399876]
24. Pavlova NN, Thompson CB. The Emerging Hallmarks of Cancer Metabolism. Cell Metab. 2016; 23:27–47. [PubMed: 26771115]
25. Puigserver P, Wu Z, Park CW, Graves R, Wright M, Spiegelman BM. A cold-inducible coactivator of nuclear receptors linked to adaptive thermogenesis. Cell. 1998; 92:829–839. [PubMed: 9529258]
26. Simoes RV, Serganova IS, Kruchevsky N, Leftin A, Shestov AA, Thaler HT, et al. Metabolic plasticity of metastatic breast cancer cells: adaptation to changes in the microenvironment. Neoplasia. 2015; 17:671–684. [PubMed: 26408259]

27. Sun P, Enslen H, Myung PS, Maurer RA. Differential activation of CREB by Ca2+/calmodulin-dependent protein kinases type II and type IV involves phosphorylation of a site that negatively regulates activity. Genes Dev. 1994; 8:2527–2539. [PubMed: 7958915]

28. Yang J, Staples O, Thomas LW, Briston T, Robson M, Poon E, et al. Human CHCHD4 mitochondrial proteins regulate cellular oxygen consumption rate and metabolism and provide a critical role in hypoxia signaling and tumor progression. J Clin Invest. 2012; 122:600–611. [PubMed: 22214851]

29. Zhang Q, Adiseshaiah P, Kalvakolanu DV, Reddy SP. A Phosphatidylinositol 3-kinase-regulated Akt-independent signaling promotes cigarette smoke-induced FRA-1 expression. J Biol Chem. 2006; 281:10174–10181. [PubMed: 16490785]

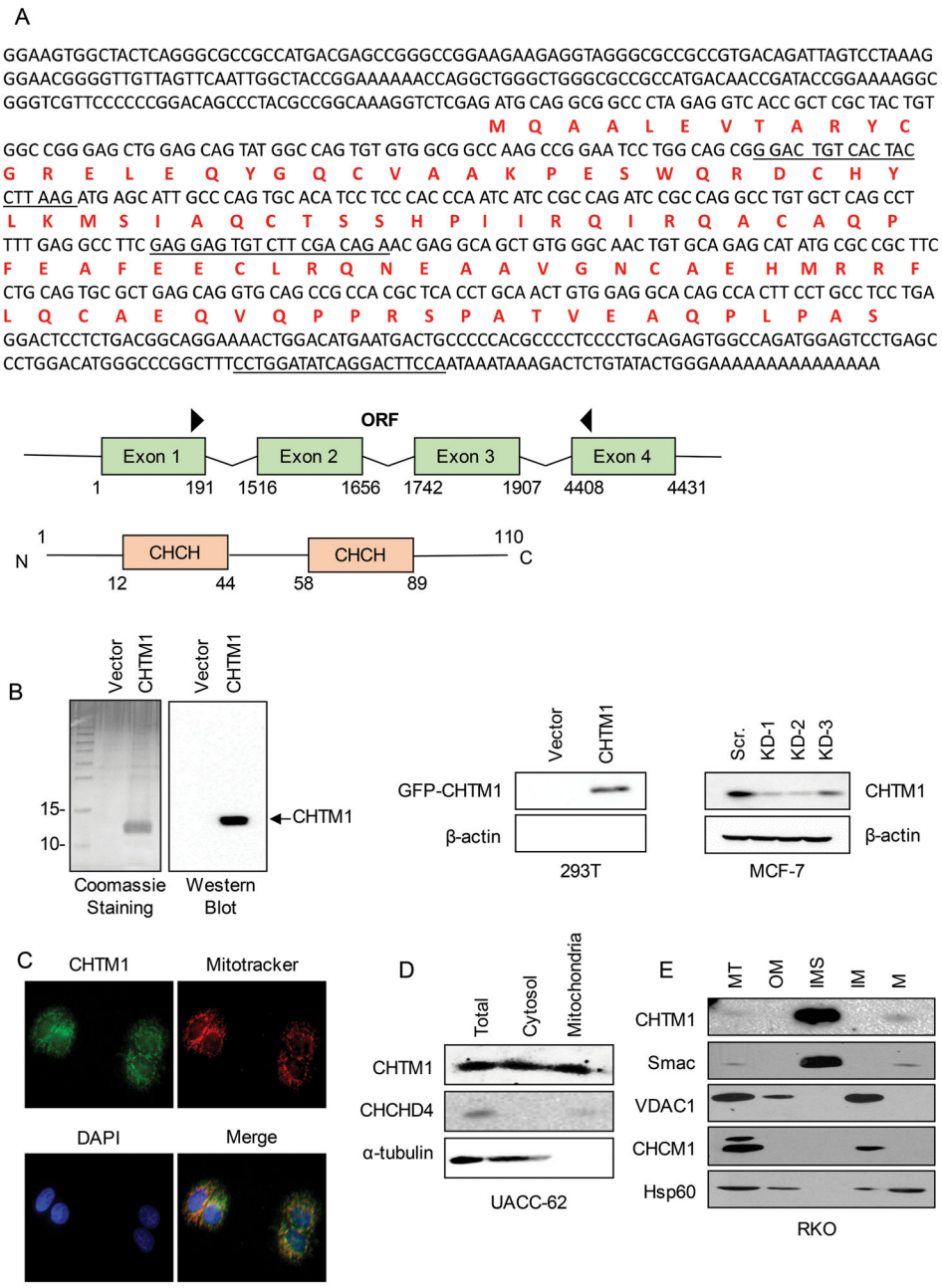

Figure 1.

(A) Upper panel, nucleotide and amino acid sequence of CHTM1. Underlined sequences indicate the targeted-sites for shRNA-based CHTM1 knockdown. Middle panel, genomic organization of CHTM1. Region between the arrows corresponds to CHTM1 open reading frame (ORF*).* Bottom panel, structural organization of CHTM1 with predicted CHCH domains. (B) Left panel, purified CHTM1 stained with Coomassie dye and then probed with purified anti-CHTM1 antibody. Middle and right panels, the anti-CHTM1 antibody detect exogenous and endogenous CHTM1 on Western blot analysis respectively. CHTM1 signals are reduced in CHTM1-knocked down cells confirming antibody specificity. Endogenous

CHTM1 expression was silenced by the lentivirus-mediated shRNA approach. The scramble shRNA construct was purchased from Addgene, Inc. (Cambridge, MA). All other shRNA constructs were purchased from Origene, MD. The three different nucleotide sequences to target the human CHTM1 used in this study were as follows: KD1, 5′-CTTAAGGTAGTGACAGTCC-3′; KD2, 5′-TCTGTCGAAGACACTCCTC-3′ and KD3, 5′-TGGAAGTCCTGATATCCAG-3′. Virus production and infection were performed per the protocol provided by Addgene. (C) Representative fluorescent photomicrographs show subcellular distribution of endogenous CHTM1 (green) in MCF-7 human breast cancer cells; cells were co-stained with mito-tracker (red) and DAPI (blue) to detect mitochondria and nuclei respectively staining (Olympus AX70, Objective 60X). (D) Western blot analyses showing subcellular distribution of endogenous CHTM1 in UACC-62 melanoma cells. (E) Western blot analyses of sub-mitochondrial fractions predominantly detect CHTM1 in the inter-membrane space of mitochondria in RKO colon cancer cells. MT : Mitochondria ; OM : Outer Membrane ; IMS : Intermembrane space ; IM ; Inner-membrane and M : Matrix.

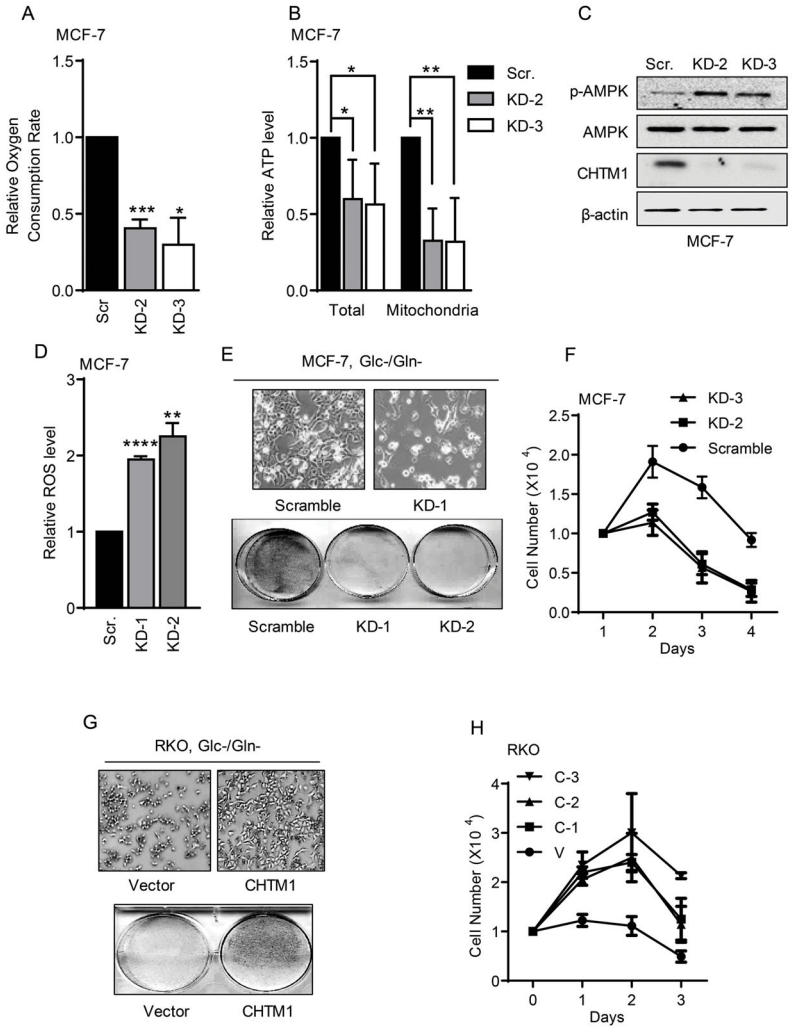

Figure 2.

CHTM1 knockdown affects mitochondrial (A) oxygen consumption. MCF-7 cells with CHTM1 knockdown or scramble knockdown were harvested by trypsinization and subjected to centrifugation at 2500 rpm. 1.5×10^6 cells were resuspended in 300 μl of growth medium for each sample and injected into the polarographic chamber for the intact cell-coupled oxygen consumption rate. and (B) ATP production in MCF-7 human breast cancer cells. (C) Western blot showing CHTM1 knockdown increases phospho-AMPK in MCF-7 cells. (D) CHTM1 increases oxidative stress in MCF-7 cells. Cells were stained with 1 μM DCF-DA a ROS sensitive dye (Invitrogen, CA) for 45 minutes at 37˚C followed by washing with Hank's balanced salt solution and fluorescence intensity measurement was done at excitation: 485 nm and emission: 530 nm using Synergy 2 micro plate reader. (E & F) CHTM1 knockdown and scrambled MCF-7 cells were grown in the absence of glucose/ glutamine (Glc/Gln) deprivation for 48h; CHTM1 knockdown cells are more sensitive to Glc/Gln deprivation compared to scramble cells. Panels E & F show phase contrast microscopy, crystal violet staining & trypan blue exclusion assay respectively. (G & H) CHTM1 overexpressing RKO colon cancer cells are less sensitive to Glc/Gln deprivation in

comparison to vector-only expressing cells. Panels G & H show phase contrast microscopy, crystal violet staining, & trypan blue exclusion assay respectively. CHTM1 overexpression using pCEP4-CHTM1 construct in RKO cells (Lower Panel H). Values represent mean ± S.E. (*error bars*) of three independent experiments. *$p < 0.05$; ** $p < 0.01$; *** $p < 0.001$.

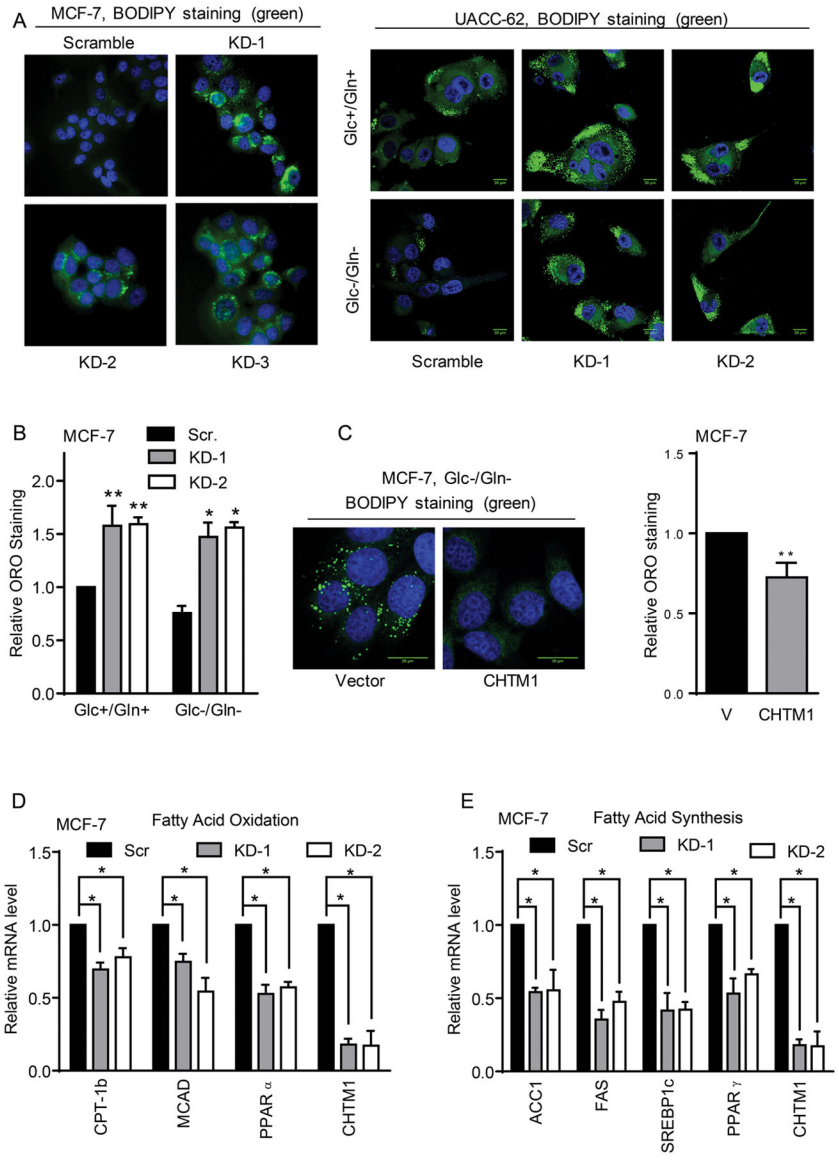

Figure 3.

CHTM1 regulates lipid metabolism. Cells were cultured in the Lab-tek II chamber slides and subjected to glucose/glutamine deprivation. Cells were then fixed with 4% paraformaldehyde for 30 minutes. Fixed cells were stained with 0.1 mg/ml BODIPY for 10 minutes and washed twice with PBS. DAPI was used for nuclear staining and slides were analyzed using a Zeiss LSM 780 confocal microscope that had the required filters. Images were processed using Image J software. (A) CHTM1 knockdown causes increase in cellular lipid content. Representative confocal images of scrambled and CHTM1 knockdown MCF-7 breast cancer cells (Olympus AX70, Objective 60X). and UACC-62 melanoma cells stained with BODIPY and DAPI are shown (Zeiss LSM 780). Scale bar represents 20 μm. Left panel, scrambled and CHTM1 knockdown MCF-7 breast cancer cells grown in complete medium. Right Panel, scrambled and CHTM1 knockdown UACC-62, melanoma cells grown in complete medium or glucose/glutamine (Glc/Gln)-deprived medium for 24h (B) Oil red O

(ORO) staining in scramble and CHTM1 knockdown MCF-7 cells grown in complete medium or in Glc/Gln-deprived medium for 24h. ORO staining shows increased lipid content in CHTM1 knockdown cells. (C) Left panel, representative confocal images of control and CHTM1 overexpressing MCF-7 cells grown in Glc/Gln-deprived medium for 24h (Zeiss LSM 780). Scale bar represents 20 μm. Right panel: Oil red O staining in CHTM1 overexpressing MCF-7 cells grown in Glc/Gln-deprived conditions for 24h show decrease in lipid content. (D) CHTM1 knockdown decreases mRNA levels of genes involved in fatty acid oxidation (CPT1b, MCAD AND PPARα). (E) CHTM1 knockdown decreases mRNA levels of genes involved in fatty acid synthesis (ACC1, FAS, SREBP1c, PPARγ). mRNA levels were analyzed by Q-PCR and the values represent SEM± of three independent experiments. Two-step quantitative real-time PCR was performed using the iScript cDNA Synthesis Kit and iQ SYBR Green super mix from Bio-Rad (Hercules, CA, USA). Specific gene values were normalized to the C(T) values of GAPDH (glyceraldehyde 3-phosphate dehydrogenase) mRNA within the same sample. The following primer sets were used: ACC1 forward: 5′-ATC CCG TAC CTT CTT CTA CTG -3′; reverse: 5′-CCC AAA CAT AAG CCT TCA CTG -3′; FAS forward: 5′-CAG GGA CAA CCT GGA GTT CT -3′; reverse: 5′-CTG TGG TCC CAC TTG ATG AGT -3′; SREBP1c forward: 5′-GGA GGG GTA GGG CCA ACG GCC T -3′; reverse: 5′-CAT GTC TTC GAA AGT GCA ATC C -3′; PPAR′ forward: 5′-GGC TTC ATG ACA AGG GAG TTT C -3′; reverse: 5′-AAC TCA AAC TTG GGC TCC ATA AAG -3′; CHTM1 forward: 5′-GAG CAG TAT GGC CAG TGT GT -3′; reverse: 5′-ACT GGG CAA TGC TCA TCT TA -3′; MCAD forward: 5′-TAC TTG TAG AGC ACC AAG CAA TAT CA -3′; reverse: 5′-TGC TCT CTG GTA ACT CAT TCT AGC TAG T -3′; PPARα forward: 5′-GGC GAG GAT AGT TCT GGA AGC -3′; reverse: 5′-CAC AGG ATA AGT CAC CGA GGA G -3′; PGC-1α forward: 5′-TGC CCT GGA TTG TTG ACA TGA -3′; reverse: 5′-TTT GTC AGG CTG GGG GTA GG -3′, CPT1b: forward: GCGCTGGAGGTGGCTTT, reverse: TCGTGTTCTCGCCTGCAAT; *$p < 0.05$.

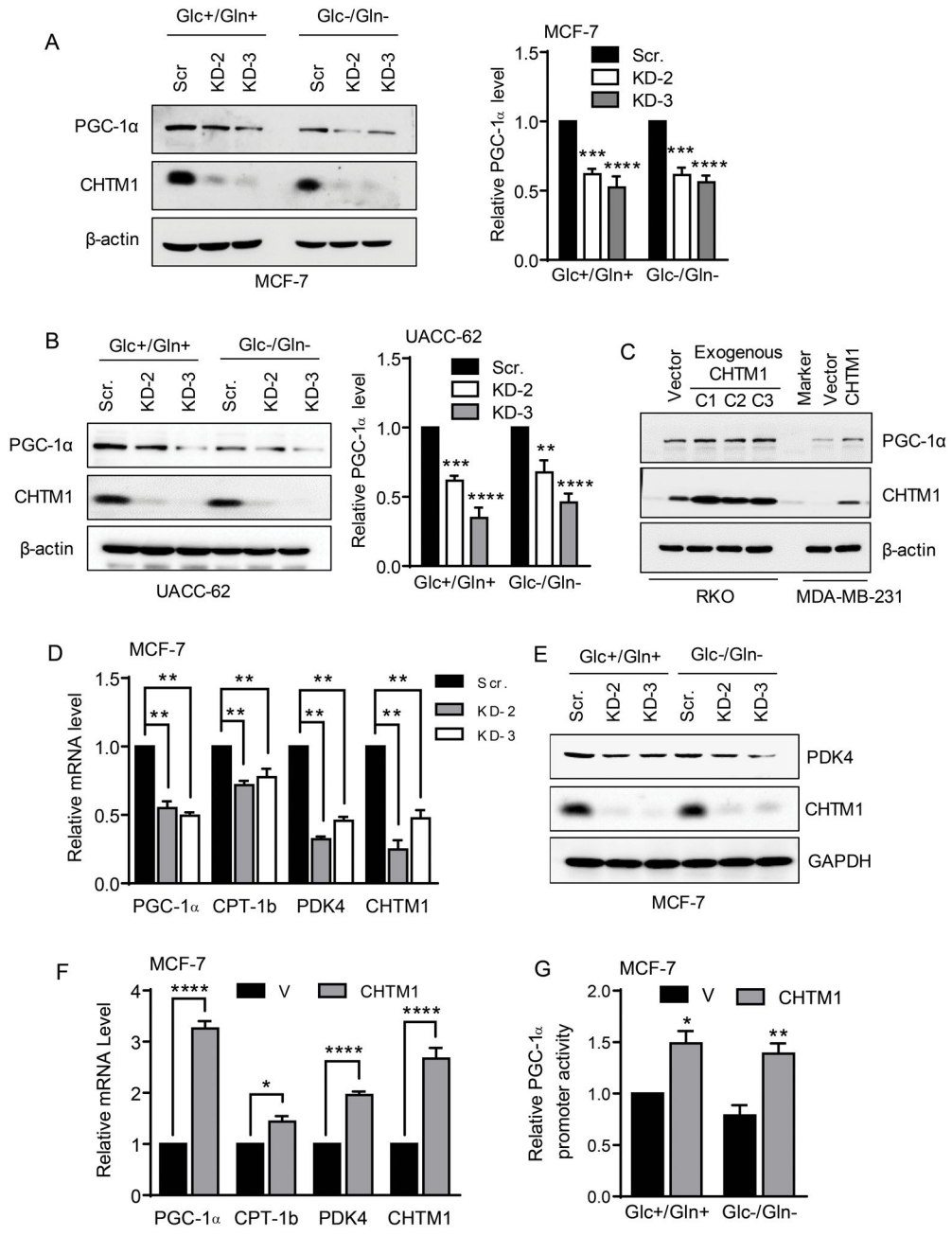

Figure 4.

CHTM1 regulates PGC-1 alpha expression and activity. (A&B) Left panels, Western blot analyses showing that CHTM1 knockdown decreases PGC-1 levels in MCF-7 cells (A) and UACC-62 cells (B) grown in complete medium or under Glc/Gln-deprived conditions for 12h. Right panels, densitometric quantification of PGC-1 alpha signals normalized to β-actin. Values are mean ±SEM of three independent experiments. (C) CHTM1 overexpression in RKO colon cancer cells and MDA-MB-231 breast cancer cells increases PGC-1 alpha levels. C1, C2 &C3 are three individual clones that exhibit stable overexpression of exogenous CHTM1. (D) CHTM1 knockdown in MCF-7 breast cancer cells downregulates

mRNA levels of PGC-1 alpha, CPT1b and PDK4. mRNA levels were analyzed by Q-PCR and the values represent SEM± of three independent experiments. The following primer sets were used PDK4 forward: 5′-CCC GCTGTCCATGAAGCAGC-3′, reverse: 5′-CCAATGTGGCTTGGGTTTCC. (E) CHTM1 knockdown downregulates PDK-4, protein levels in MCF-7 breast cancer cells grown in complete medium or in Glc/Gln-deprived medium for 12h. (F) PGC-1 alpha, CPT-1b and PDK4 mRNA levels are increased in CHTM1 overexpressing MCF-7 cells. mRNA levels were analyzed by Q-PCR and the values represent SEM± of three independent experiments (G) Exogenous expression of CHTM1 increases PGC-1 alpha promoter activity in complete medium or in Glc/Gln-deprived medium for 12h. MCF-7 breast cancer cells were transiently transfected with the indicated vectors for 24h by using TransIT-LT1 transfection reagent (Mirus, Madison, WI) according to manufacturer's protocol. Transfected cells were Glc/Gln-deprived medium for 12h. Cells were harvested, washed and lysed, followed by centrifugation at 16,000 g for 30 minutes. The luciferase activity was measured using 50μg of total protein corresponding to each sample by a luminometer (LUMAT LB9507, Berthold Technologies, Germany). MCF-7 cells were co-transfected with PGC-1 alpha promoter luciferase construct either with vector control or CHTM1 expression vector for 48h. *$p < 0.05$; ** $p < 0.01$; *** $p < 0.001$; **** $p < 0.0001$.

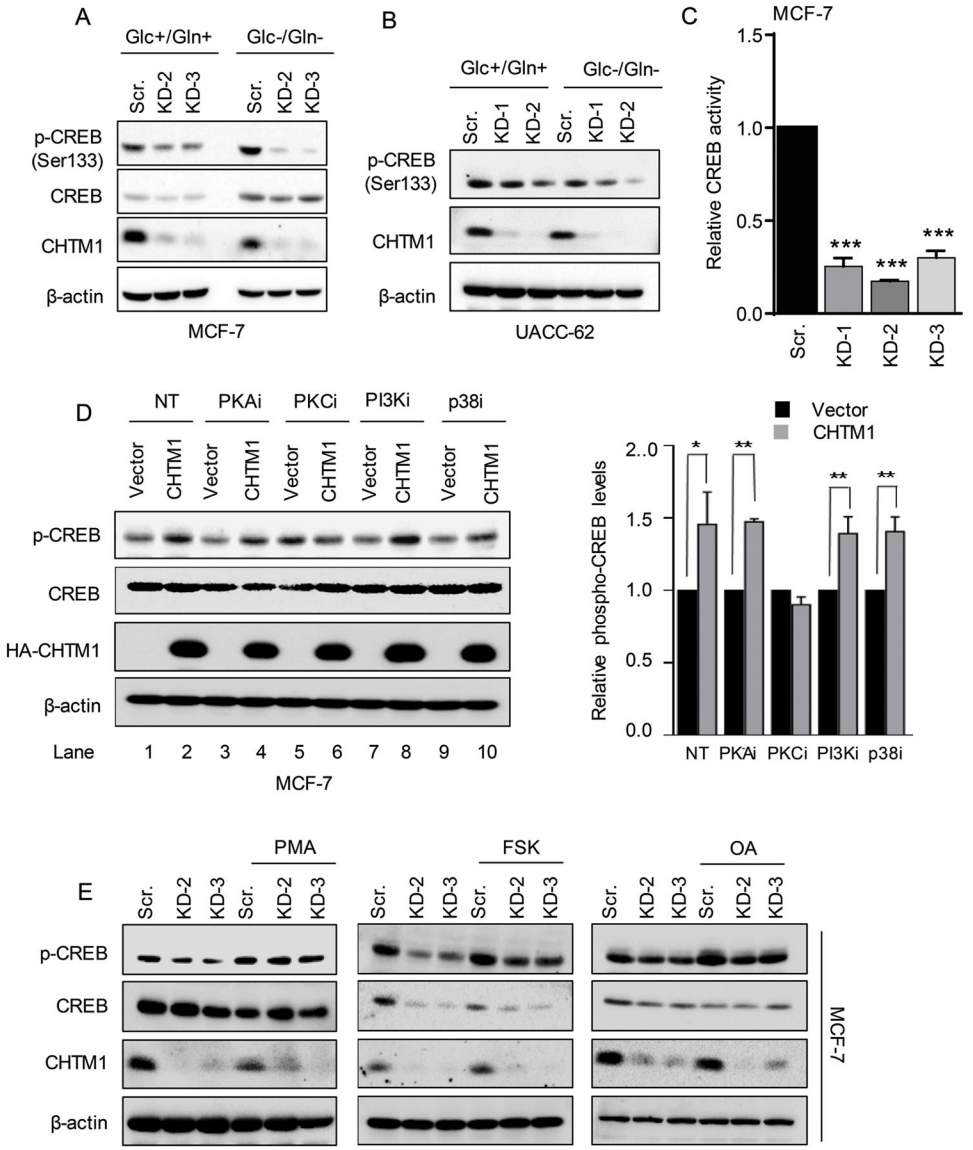

Figure 5.

CHTM1 regulates CREB phosphorylation via PKC. (A&B) Western blot analyses showing decreases in CREB phosphorylation in CHTM1 knockdown MCF-7 cells (A) and UACC-62 cells (B) grown in complete medium or Glc/Gln-deprived medium for 12h. (C) CHTM1 knockdown reduces CREB activity. Scrambled or CHTM1 knockdown MCF-7 cells were transfected with CREB DNA binding domain-luciferase construct for 48h. Promoter luciferase analyses were performed as described in Materials and methods section. Results shown are the relative luciferase amounts for CREB promoter activity and the values represent SEM± of three independent experiments. (D) PKC inhibitor blocks CREB phosphorylation in CHTM1 overexpressing MCF-7 cells. Cells were transiently transfected with vector-only or CHTM1 expression construct and grown under Glc/Gln-deprived conditions for 12h followed by Glc/Gln stimulation for 1h in the presence or absence of various kinase inhibitors- 10μM PKI (PKA), 10μM G06983 (PKC), 50μM LY294008 (PI3K)

and 30μM SB203580 (p38). Left panel, Western blot analyses; right panel, densitometric quantification showing that exogenous CHTM1 increases CREB phosphorylation (lanes 1&2) that is blocked by and PKC inhibitor (lanes 5&6). (E) PKC activation by 1 μM PMA rescues prevents decreases in CREB phosphorylation in the CHTM1 knockdown MCF-7 cells, whereas PKA activator forskolin and oleic acid were unable to do so. *$p < 0.05$; ** $p < 0.01$; *** $p< 0.001$.

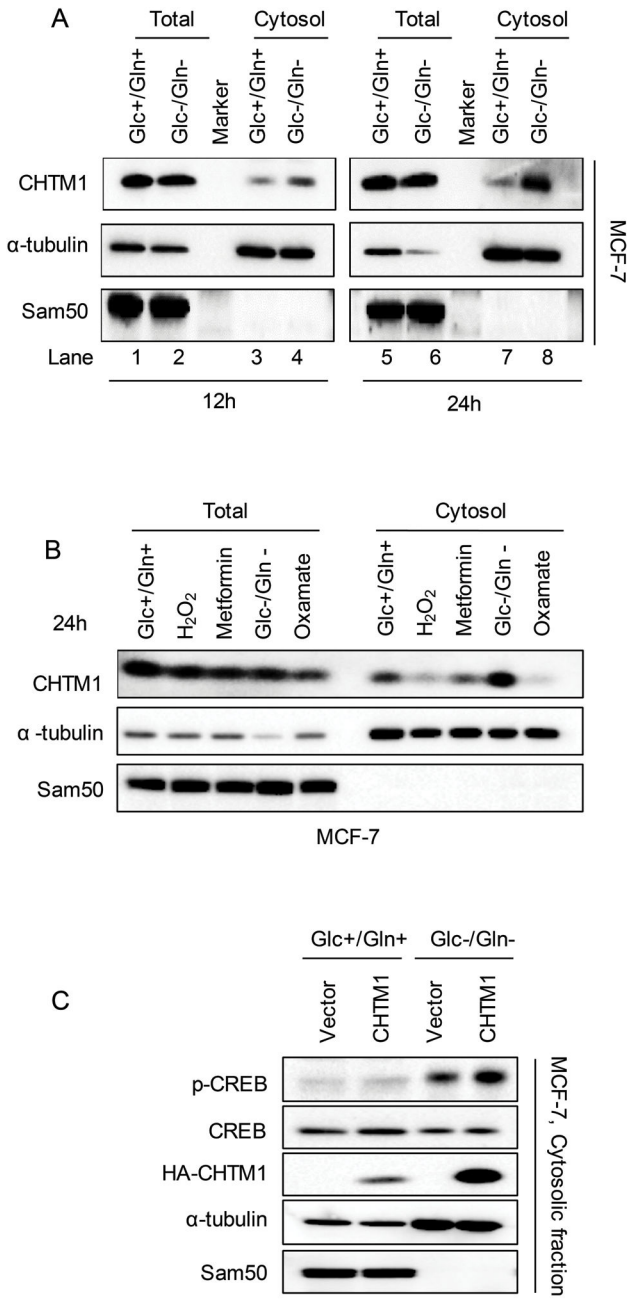

Figure 6.

Glc/Gln deprivation regulates cellular distribution of CHTM1. (A) Western blot analyses showing increased cytosolic levels of CHTM1 in MCF-7 cells grown under Glc/Gln-deprived conditions for 12h (left panel) and 24h (right panel). (B) MCF-7 breast cancer cells were grown in completed medium and treated with 25 μM hydrogen peroxide (H_2O_2), 10 mM metformin and 80 mM oxamate for 24h, or grown in Glc/Gln-deprived conditions for 24h. Western blot analyses showing increase in cytosolic levels of CHTM1 only under Glc/Gln-deprived conditions for 24h. (C) Western blot analysis showing increase in cytosolic

levels of CREB in CHTM1 overexpressing MCF-7 cells grown under Glc/Gln-deprived conditions for 12h.

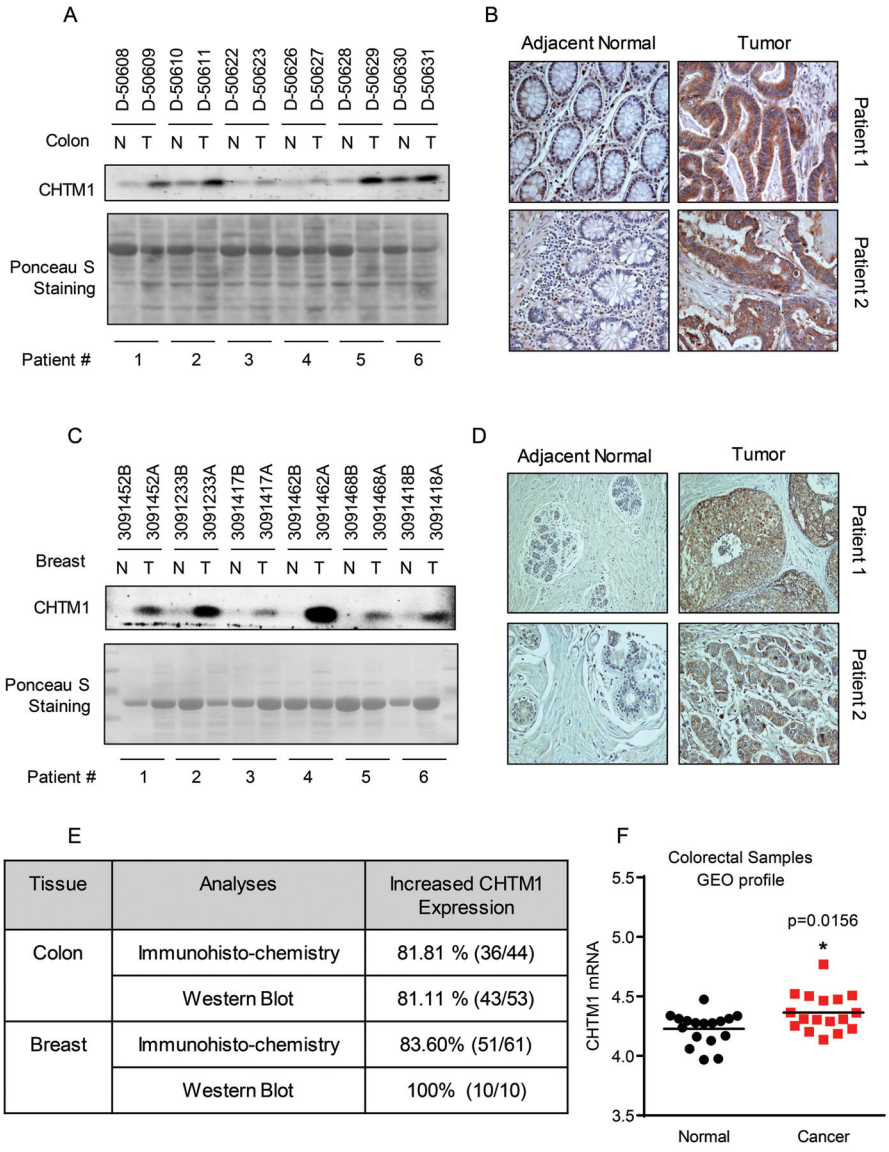

Tissue	Analyses	Increased CHTM1 Expression
Colon	Immunohisto-chemistry	81.81 % (36/44)
	Western Blot	81.11 % (43/53)
Breast	Immunohisto-chemistry	83.60% (51/61)
	Western Blot	100% (10/10)

Figure 7.

CHTM1 levels are deregulated in human cancers. (A) Representative Western blot showing CHTM1 levels are increased in tumor (T) tissue samples from colon cancer patients compared to corresponding matched normal (N) tissues. Samples were obtained from Cooperative Human Tissue Network (CHTN), an NCI-supported network. Frozen tissue samples were shipped on dry-ice and stored at -80˚C. (B) Immunohistochemical staining of CHTM1 in representative patient-derived matched normal and tumor tissues from colon cancer patients. Brown color indicates CHTM1 specific staining and blue color indicates hematoxylin (Olympus AX70, Objective 20X). Samples were purchased from Biomax (Rockville, MD) as formalin-fixed, paraffin-embedded tissue array slides. Slides were shipped and stored at room temperature. (C) Representative western blot showing CHTM1 levels are increased in tumor (T) tissue samples from breast cancer patients compared to corresponding matched normal (N) tissues. Samples were obtained from CHTN. Frozen

tissue samples were shipped on dry-ice and stored at -80˚C. (D) Immunohistochemical staining of CHTM1 in representative patient-derived matched normal and tumor tissues from breast cancer patients (Olympus AX70, Objective 20X). Samples were purchased from Biomax as formalin-fixed, paraffin-embedded tissue array slides. Slides were shipped and stored at room temperature. (E) Summary of results showing CHTM1 levels are increased in colon and breast cancer samples when compared to corresponding matched normal tissues from multiple patients. (F) Microarray data in GEO database showing that CHTM1 mRNA levels are increased in colon cancers compare to normal tissues. Values represent 17 normal and colon cancer tissue samples. GEO data ID: GDS4382. Each symbol represents an individual sample. p=0.01156.

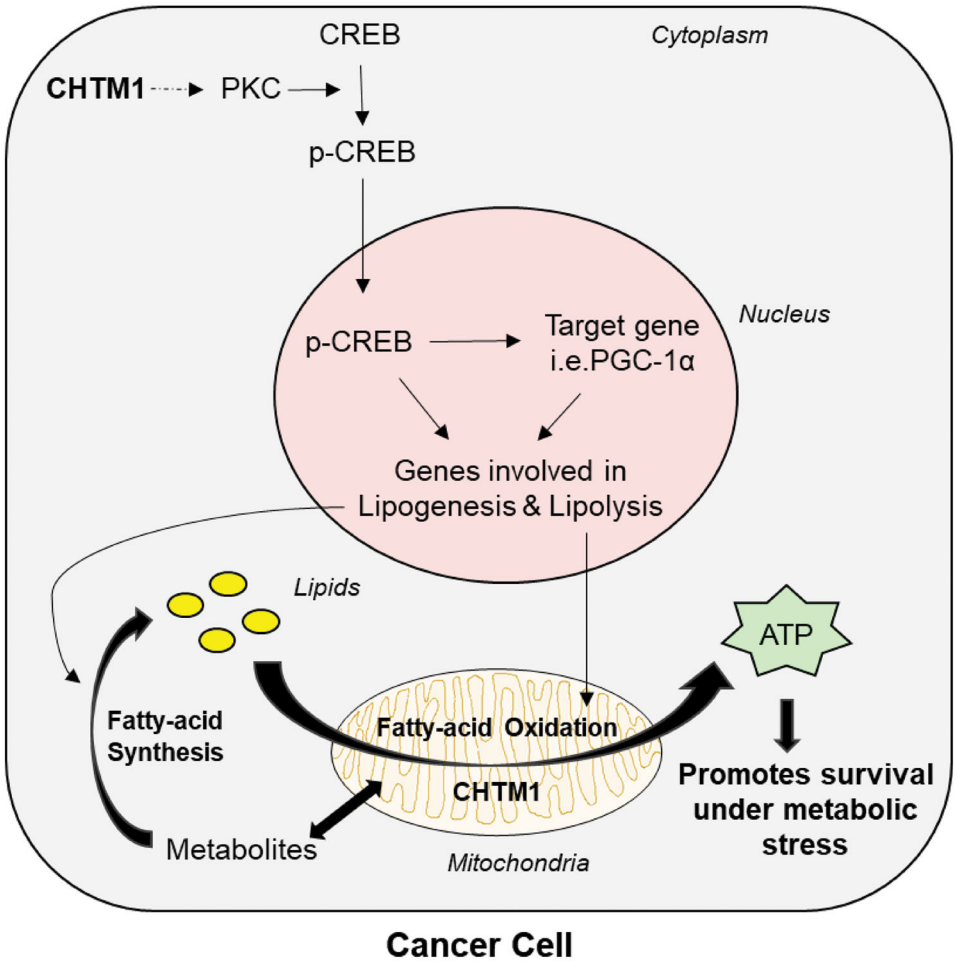

Figure 8.

Proposed model depicting the function of CHTM1as a novel modulator of metabolic stress (glucose/glutamine deprivation). Under glucose and glutamine-deprived condition, CHTM1 induces CREB-phosphorylation possibly via PKC. Phosphorylated-CREB enhances transcription of downstream targets including PGC-1 alpha, which further modulates the transcription of genes involved in lipogenesis and lipolysis. Under metabolic stress, CHTM1 regulates mitochondrial activity and induces fatty acid oxidation and therefore, generating more ATP for cancer cell survival. As a feedback response to increased lipolysis, lipogenesis is also increased. Overall, in CHTM1-proficient cancer cells, CHTM1 confers protection in response to metabolic stress by regulating lipid metabolism and PGC-1α-CREB-PKC axis. Conversely, CHTM1 deficiency increases cancer cell sensitivity to metabolic stress.